C.E. SACLAY
DSM

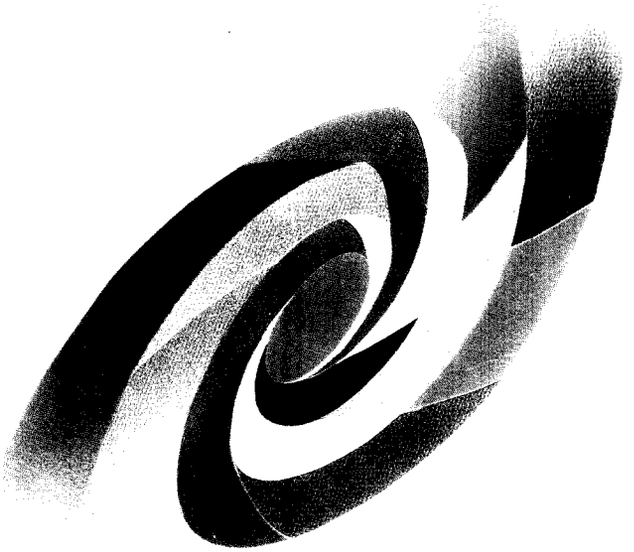

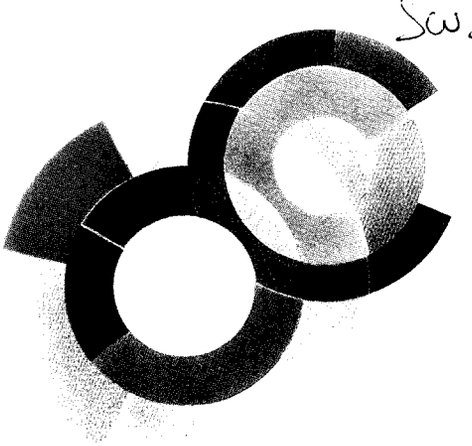

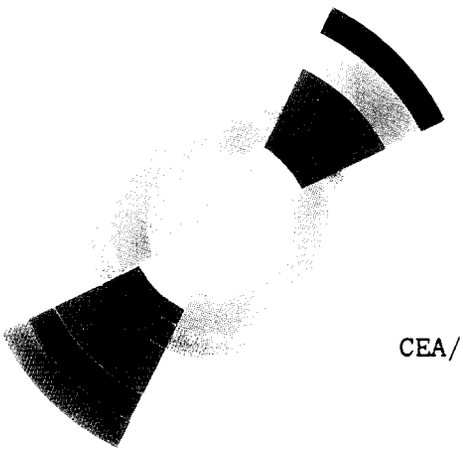

CEA/DAPNIA/SPhN 94 63 11/1994

MULTIFRAGMENTATION STUDIED WITH INDRA

Ch.O. Bacri, B. Borderie, J.L. Charvet,
R. Dayras, O. Lopez, A. Ouatizerga,
M.F. Rivet, G. Auger, A. Benkirane,
B. Berthier, J. Benlliure, R. Bougault,
P. Box, R. Brou, C. Le Brun, Y. Cassagnou,
A. Chbihi, J. Colin, D. Cussol, A. Demeyer,
D. Durand, P. Ecomard, E. de Fillipo,
P. Eudes, A. Genoux-Lubin, D. Gourio,
D. Guinet, L. Lakehal-Ayat, P. Lautesse,
P. Lautridou, J.L. Laville, L. Lebreton,
J.F. Lecolley, A. Lefèvre, R. Legrain,
M. Louvel, N. Marie, V. Métivier, L. Nalpas,
M. Parlog, J. Peter, E. Plagnol, E. Pollacco,
J. Pouthas, A. Rahmani, R. Regimbart,
T. Reposeur, F. Saint-Laurent, M. Squalli,
J.C. Steckmeyer, B. Tamain, L. Tassan-Got,
E. Vient, C. Volant, J.P. Wieleczko

DAPNIA

Le DAPNIA (**D**épartement d'**A**strophysique, de physique des **P**articules, de physique **N**ucléaire et de l'**I**nstrumentation **A**ssociée) regroupe les activités du Service d'Astrophysique (SAp), du Département de Physique des Particules Elémentaires (DPhPE) et du Département de Physique Nucléaire (DPhN).

Adresse : DAPNIA, Bâtiment 141
CEA Saclay
F - 91191 Gif-sur-Yvette Cedex

Exposé invité à "Tours Symposium on Nuclear Physics II"

Tours, France

du 30 août au 02 septembre 1994

Invited talk to the Tours Symposium on Nuclear Physics II,
August30- September 2, 1994

MULTIFRAGMENTATION STUDIED WITH INDRA.

Ch.O. BACRI[a], B. BORDERIE[a], J.L. CHARVET[b], R. DAYRAS[b], O. LOPEZ[c], A. OUATIZERGA[a], M.F. RIVET[a]

G. AUGER[d], A. BENKIRANE[d], B. BERTHIER[b], J. BENLLIURE[d], R. BOUGAULT[c],P. BOX[a], R. BROU[c], C. LE BRUN[c], Y. CASSAGNOU[b], A. CHBIHI[d], J. COLIN[c], D. CUSSOL[c], A. DEMEYER[f], D. DURAND[c], P. ECOMARD[d], E. DE FILLIPO[b], P. EUDES[e], A. GENOUX-LUBAIN[c], D. GOURIO[e], D. GUINET[f], L. LAKEHAL-AYAT[a], P. LAUTESSE[f], P. LAUTRIDOU[e], J.L. LAVILLE[e], L. LEBRETON[f]. J.F. LECOLLEY[c], A. LEFEVRE[d], R. LEGRAIN[b], M. LOUVEL[c], N. MARIE[d], V. METIVIER[c], L. NALPAS[b], M. PARLOG[a], J. PETER[c], E. PLAGNOL[a], E. POLLACO[b], J. POUTHAS[d], A. RAHMANI[e], R. REGIMBART[c], T. REPOSEUR[e], F. SAINT-LAURENT[d], M. SQUALLI[a], J.C. STECKMEYER[c], B. TAMAIN[c], L. TASSAN-GOT[a], E. VIENT[c], C. VOLANT[b], J.P. WIELEZKO[d].

a : IPN, IN2P3-Université Paris Sud, 91406 Orsay, France
b : DAPNIA, CEN Saclay, 91191 Gif sur Yvette, France
c : LPC Caen, 14050 Caen Cedex, France
d : GANIL, BP5027, 14021 Caen, France
e : LPN, Nantes, 44072 Nantes Cedex, France
f : IPN Lyon, 69622 Villeurbanne Cedex, France

ABSTRACT

After a brief description of the INDRA detector and of our scientific program, some first results will be discussed, on the Ar + Ni system for incident energies ranging from 32 to 95 MeV/A. A slow evolution from incomplete fusion up to a total vaporization of the system could be deduced from IMF, Z, and Z_{max} distributions. A threshold of excitation energy to vaporize the system is deduced.

1. Introduction

It is now well established that multi-fragment emission is an important decay channel for strongly excited nuclear systems, formed in heavy ion collisions at intermediate bombarding energies ($10 \leq E_i \leq 100$ MeV/A) [1-6]. In order to disentangle between the different scenarii, precise and systematic experimental measurements are clearly needed to characterize and to study this disintegration process. The 4π multidetector INDRA was designed for such studies and has been available for experiments since the beginning of 1993.

In the first part of this paper, the detector will be briefly described and our scientific program presented. Then, some results will be discussed on the Ar+Ni system at different incident energies.

2. The detector and the scientific program

2.1. The detector

Indra is a 4π detector for charged products [7,8]. It has an axial symmetry and its high granularity (336 independent modules organized in 17 rings) associated to its geometrical efficiency (90% of 4π) allows a very efficient detection of high multiplicity events. The first ring is made of 12 rapid plastic phoswiches and was designed to accept high counting rate, since it covers forward angles (2°-3°). From 3° to 45°, each module is a three member telescope made of an ionization chamber (for the detection of slow fragments), a 300 μm silicon detector (for the detection of fast fragments), and a CsI crystal (for the detection of fast fragments and of light charged particles). At larger angles (45°-176°), fast heavy ions are not expected and the silicon detector was removed from the module. Very low energy threshold have been obtained as well as charge resolution up to Z=60. For light particles (Z≤ 3), a mass separation is also achieved.

The treatment of the signal is performed through specifically designed modules, most of which being in the new VXIbus standard. This electronics allows to cover a huge dynamics (from 1 MeV to 5 GeV for the silicon detectors) and to fully remote control the detector.

2.2. The scientific program

Our program is mainly devoted to an exhaustive study of the decay of hot nuclear systems by multifragmentation, that is the search for the transition from a sequential decay to a simultaneous one. Some theoretical investigations propose different models for such a process [9].

Dynamical calculations predict multifragmentation as the result of a strong compression phase in the early stage of the reaction, for the more central collisions [10-12]. The hot system then expands and is predicted to enter a mechanical instability region (the so-called spinodal region), connected to the existence of a liquid-gas phase transition for nuclear matter. If the system remains long enough in this region, a prompt multifragment disassembly is then expected. Such a process, for light systems, is predicted to occur for intermediate incident energies (~ 40 - 60 MeV/A). On the other hand, and for very heavy systems, Coulomb instabilities are predicted to enhance the expansion. Then, multifragmentation could occur after a more gentle compression step, and consequently, at lower energies (~ 25 MeV/A)[13,14]. Exotic shapes such as bubbles, donuts, or disks are then expected to be formed before the multi-fragment emission[15,16].

Statistical models are also proposed by J.P.Bondorf et al.[17] and by D.H.E.Gross et al.[18] which predict an increase of the fragment emission probability with increasing energies.

The second part of our program consists in nuclear flow studies. A description of this program will be found in the D.Cussol et al. contribution to this conference.

Up to now, two sets of experiments were performed. The first one ended 15 months ago, while the second one just ended at the end of July 1994. We choose to study the problem of multifragmentation by means of four different approaches which are summarized in Table 1. The first one consists in varying the size of symmetric systems, at dif-

ferents energies. It is then possible to study the importance of the mean field by studying all differences from scaling laws, when the size of the system changes. The second approach consists in studying different systems with the same total mass in order to learn about entrance channel effects. The study of light systems can be made on a large range of incident energies at Ganil. For the Ni + Ni system, a complementary study from ~150

Size effects	Energy (MeV/A)	**Entrance channel effects**	Energy (MeV/A)
^{36}Ar + KCl	32, 40, 52,74	^{129}Xe + Sn	25, 32, 40, 45, 50
^{129}Xe + Sn	25, 32, 39, 45, 50		
^{58}Ni + ^{58}Ni	32, 40, 52,63, 74, 82, 90	^{58}Ni + ^{197}Au	32, 52, 63, 74, 82, 90
^{181}Ta + ^{197}Au	33,39		
Heavy systems - gentle compression	Energy (MeV/A)	**Light systems - strong compression Vaporization - Flow meas.**	Energy (MeV/A)
^{155}Gd + ^{238}U	36	^{36}Ar + ^{58}Ni	32, 40, 52, 63, 74, 84, 95
^{181}Ta + ^{238}U	33,39	^{58}Ni + ^{58}Ni	32, 40, 52,63, 74, 82, 90 → 400 with Fopi at Sis
^{238}U + ^{238}U	24		

Table 1 : The systems studied with INDRA.

to 400 MeV/A with the Fopi detector will complete results obtained at lower energies at Ganil. Moreover, the large range of incident energies allows to make a complete study of the flow of nuclear matter. At last, very heavy ions systems are studied in order to use Coulomb instabilities to initiate multifragmentation.

In order to sample the first obtained results, only the Ar + Ni system will be discussed in the following, because the covered energy range allows to follow the evolution of reaction mechanisms from 32 up to 95 MeV/A.

In order to reduce random coincidences, a very thin target (193 $\mu g/cm^2$) and a very low beam intensity (~ 2-3 10^7particles per second) was used. Moreover, a 35 kV high voltage was applied on the target to reduce the noise coming from the electrons of the target. Events were registred when at least 3(4) modules fired for the energies 32-74 (84-95) MeV/A. In these conditions, acquisition dead time was around 20%.

Up to now, all identifications in charge and, for light particles, in mass are available. The energy calibrations will be available very soon.

3. Experimental results

3.1. Event selection

The analysis of data obtained with a 4π detector needs a careful selection of the "well detected events". Usually, a selection about the total detected charge (Z_{tot}) is performed but it leads to filter the physics with the detector efficiency. Another selection will be then performed.

An important observable in the study of multifragmentation is the number of Intermediate Mass Fragments (called IMF in the following), defined as fragments with $Z \geq 3$. Then the selected events will be those for which the probability to detect all IMF is greater than or equal to 90%.

A very simple procedure was performed in order to search for those "well detected events", assuming a unique hypothesis : the probability to not detect a particle is the same whatever are its charge and its production angle. First, we have defined different bins of multiplicity for all events with a total detected charge greater than or equal to 18 (events with a total charge less or equal to the projectile charge are indeed very badly detected). It is then possible to determine the Z distribution of these events for each bin. Events were then built according to the corresponding experimental Z distribution , and so until the total available charge is obtained. For each simulated event, it is then possible to attribute a calculated multiplicity. This procedure was repeated 10 000 times for each multiplicity bin. At last, in order to find again the initial experimental multiplicity, some particles are considered as not detected. The probability to lose an IMF is then determined.

In fact, for the Ar + Ni system, and for all the studied energies, we have found this criterion to be equivalent to take a total detected charge greater than or equal to 41, that is nearly 90% of the total available charge. This could mean that INDRA is well suited for studying collisions for which the IMF distribution is an important observable, since our selection keeps indeed events for which the maximum information is available.

3.2. Multiplicity distributions

In order to study the effects of such a selection upon the detected events, contour plots of charged product multiplicity versus the total detected charge are shown in Fig.1. The general trend is an increase of the maximum multiplicity with increasing energy, indicating an increase of the violence of the collision. Peripheral dissipative binary collisions can be observed at low multiplicity : events for which the target-like and the projectile-like fragment were not detected can be recognized at low Z_{tot} , and those for which only the target-like fragment was missed can be seen for $Z_{tot} \sim 18$.

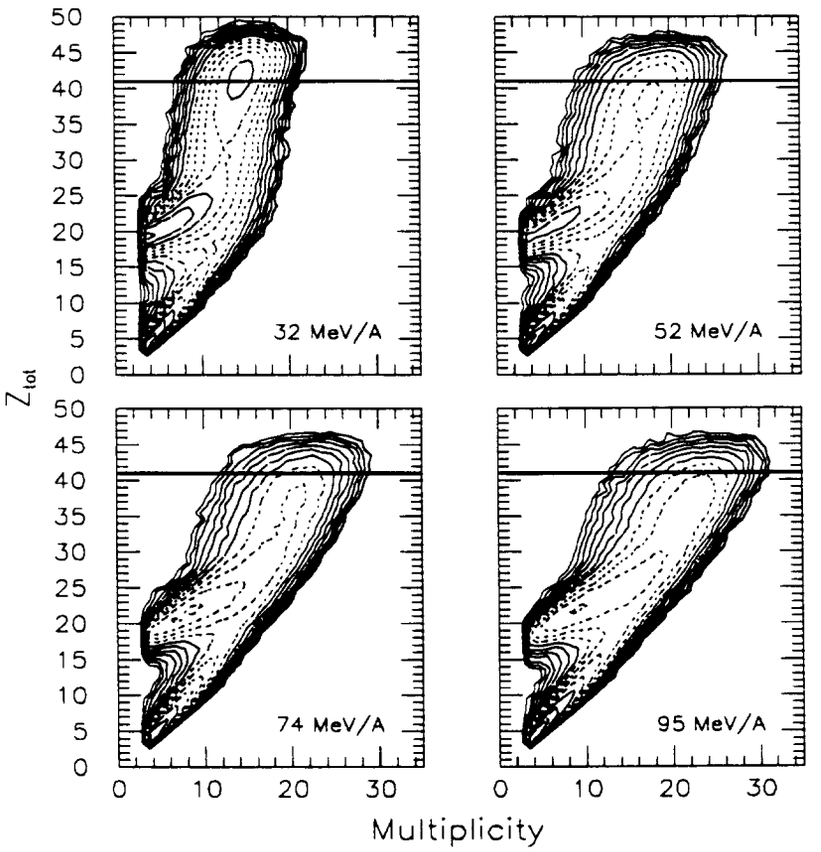

Figure 1 : Z_{tot}- Multiplicity plot for differents energies for the ^{36}Ar + Ni system.

The selection with $Z_{tot} \geq 41$ is represented by the horizontal line. It should be noticed that this selection does not select a particular class of events but events over a large multiplicity range, which do not only correspond to violent collisions. This means that a

large variety of mechanisms can be studied with such a selection. To avoid mixing different type of collisions, we have performed a rough evaluation of the impact parameter. First, using a calibration of the beam intensity (corrected for the dead time of the acquisition system), we have determined the relationship F between the cross section and the counting rate during the experiment. This relationship was verified by a comparison between the found cross section for a minimum triggered run (one event is recorded if at least one module of INDRA is fired), and the total cross section σ calculated by the use of the systematics of Kox et al.[19]. Taking into account all the detected events (that is with no selection on Z_{tot}), we have then defined differents slices in multiplicity, starting from the higher one. The impact parameter b is given by $\sigma = F(n) = \pi b^2$, where n is the total number of events integrated from the maximum multiplicity to the selected one. For all selected events ($Z_{tot} \geq 41$), three impact parameter ranges have been defined : $0 \leq b \leq 3$ fm for the more violent collisions, $3 < b \leq 6$ fm for intermediate impact parameters, and $6 < b \leq 7$ fm, for the more peripheral collisions. These values have to be compared to the maximum impact parameter for the Ar + Ni system, which is ~10 fm.

3.3. IMF distributions

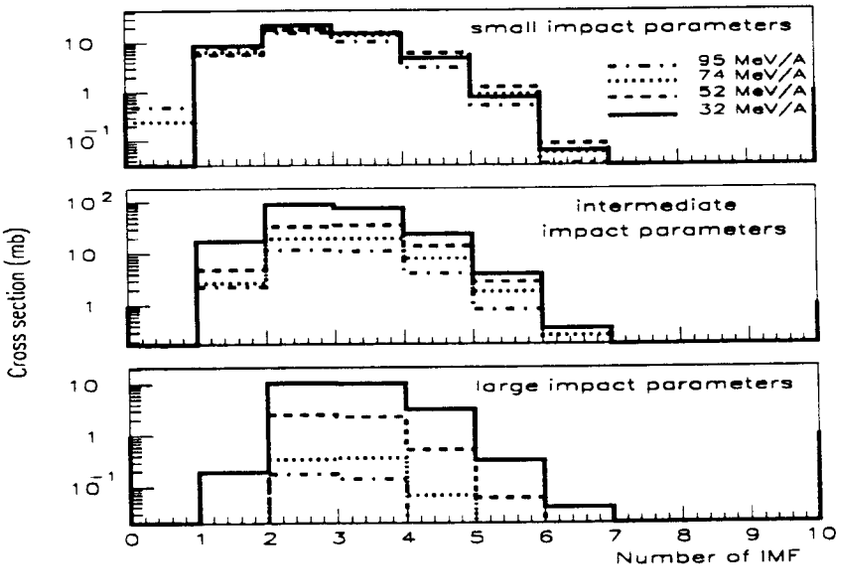

Figure 2 : Evolution with the incident energy of IMF distributions for different impact parameters bins for the ^{36}Ar + Ni system; $Z_{tot} \geq 41$.

Figure 2 displays the evolution of the IMF distributions with incident energy and for different ranges of impact parameters. It is interesting to note that the overall shape of these distributions as well as their mean value are very similar for a given class of collision . This result could confirm results obtained by D. Benchekroun et al.[20] who showed that IMF multiplicity does not reflect the excitation energy stored in the system. One can also remark that for the less violent collisions (large impact parameter range), the IMF production cross section decreases when the energy increases. This is probably due to the fact that for high incident energies, IMF distributions are more concentrated in the forward direction and then, the probability not to detect one IMF increases. At last, it is interesting to note that, above 52 MeV/A, there are some events for which no IMF are produced in central collisions (see section 3.6) !...

3.4. Charge distributions

The size of these IMF can be deduced from the Z distributions, as shown in Fig. 3. The overall shape of these distributions are quite the same for all energies and all impact parameter ranges : a steep decrease by a factor ~10 in the production cross section between Z=2 and Z=3, followed by a kind of shoulder which becomes less pronounced when the energy increases. The largest Z decreases with the energy. Comparing Fig. 2 and Fig. 3, one can deduce that, for the more violent collisions, the IMF size decreases when the energy increases. Nevertheless, fragments as large as Z=20 are produced in the more violent collisions, at 95 MeV/A !

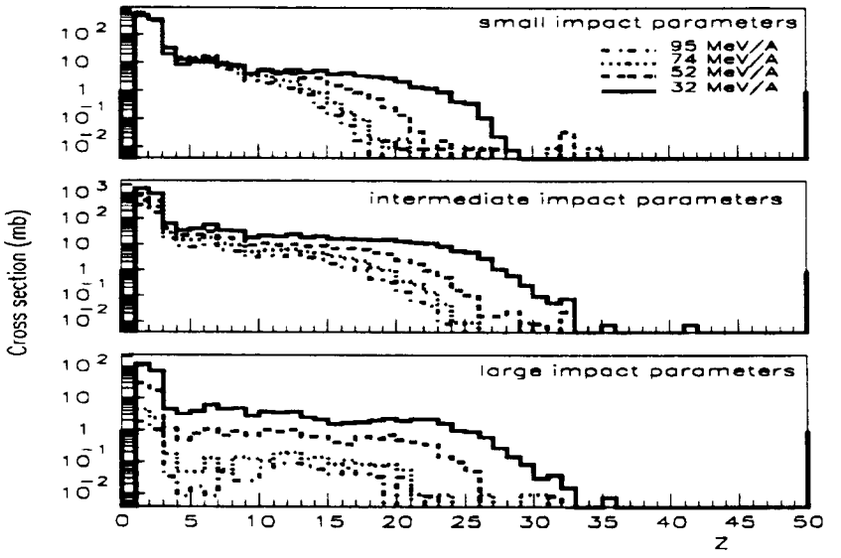

Figure 3 : Evolution with the incident energy of Z distributions for different impact parameters bins for the ^{36}Ar + Ni system ; $Z_{tot} \geq 41$.

3.5. Charge distributions of the largest fragment

The evolution of the charge of the largest fragment, Z_{max} , is displayed in Fig. 4. Once again, the overall shape of the distributions seems to be the same for all energies and all impact parameters even if the most probable value of Z_{max} decreases whith increasing energies. Nevertheless, it is interesting to note that for the more violent collisions, and by opposition with other ones, the production cross section of the smallest fragments increases with incident energy. If the number of IMF remains constant with increasing energies (see Fig. 2), their size indeed decreases. This reflects probably the onset of the vaporization of the system, since events for which the larger fragment has a charge Z=2 are produced for incident energies larger than or equal to 52 MeV/A.

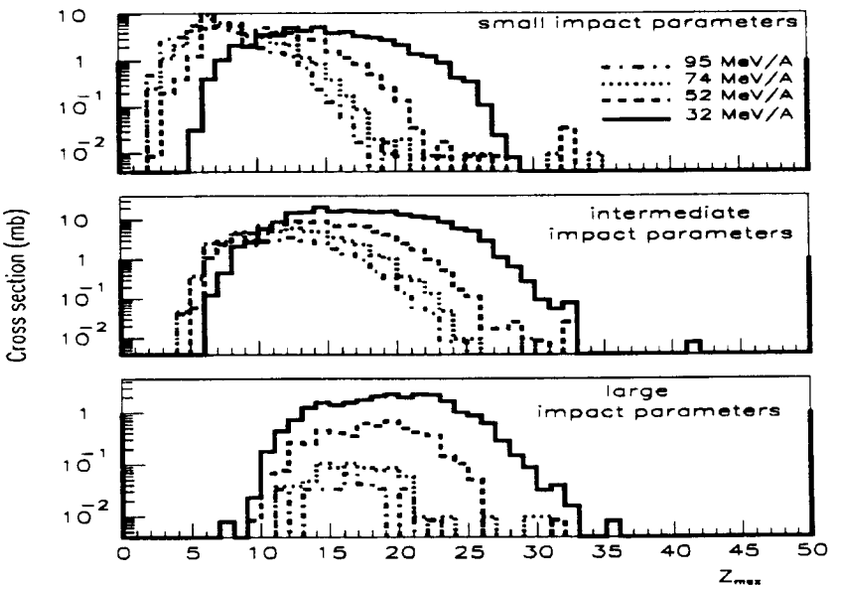

Figure 4 : Evolution of the size of the largest fragment with incident energy, and impact parameters, for the ^{36}Ar + Ni system ; $Z_{tot} \geq 41$.

3.6. Vaporization events

Vaporization events are defined as events for which only light charged particles ($Z \leq 2$) are detected. It is then important to remember that our selection of the "well

detected events" selects all events for which the probability to detect all IMF ($Z \geq 3$) is greater than or equal to 90% (see section 3.3).

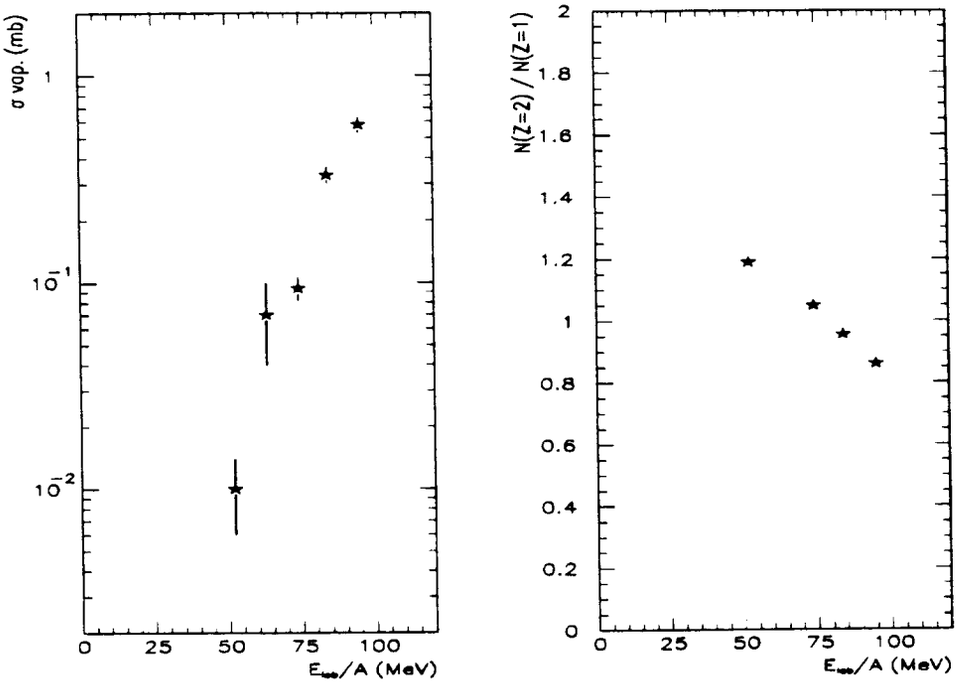

Figure 5 : Evolution of the production cross section of vaporization events (left part), and of the ratio Helium isotopes / Hydrogen isotopes , with the incident energy.

The evolution of the production of such events is shown on the left part of Fig. 5. No vaporization events have been detected below 52 MeV/A. The steep increase of the vaporization cross section can be related to the evolution of the mean ratio Z=2 / Z=1 : Z=2 particles dominate over Z=1 particles when the energy decreases (right part of Fig.5). This is probably due to energetic considerations, since the production of an alpha particle is energetically more favorable than the production of a proton. Moreover, one could notice that ^{36}Ar can be viewed as a cluster of 9 α particles and ^{58}Ni as 14 α particles and 2 neutrons. In order to evaluate a threshold for the production of vaporization events, we tried to calculate an excitation energy associated to the detected events (completed with neutrons and protons, until the total available charge Z_{tot}= 46 was attained) . The following formula was used :

$$E^* = (Q + V_c + M_{corr}.E_k) / A_{tot}$$

where M_{corr} is the multiplicity of the completed event. The mean value of the mass balance, Q, was calculated and is reported in Fig.6 as full circles. V_c , the Coulomb energy is the needed energy to get a compact configuration from particles coming from the infinity. Full squares represent in Fig.6 the mean value $< Q+V_c >$. The kinetic energy E_k

of the particles is not yet known and was evaluated as thermal energy : E_k = 2 T. 7 MeV seems to be a reasonable estimation of the temperature since it is the saturation temperature for the Ar+Al and Ar+Ag systems [21]. The resulting excitation energy is reported as open squares in Fig.6 and have to be compared with the available energy (full stars). A threshold of ~12 MeV/A for the production of vaporization events can be then deduced.

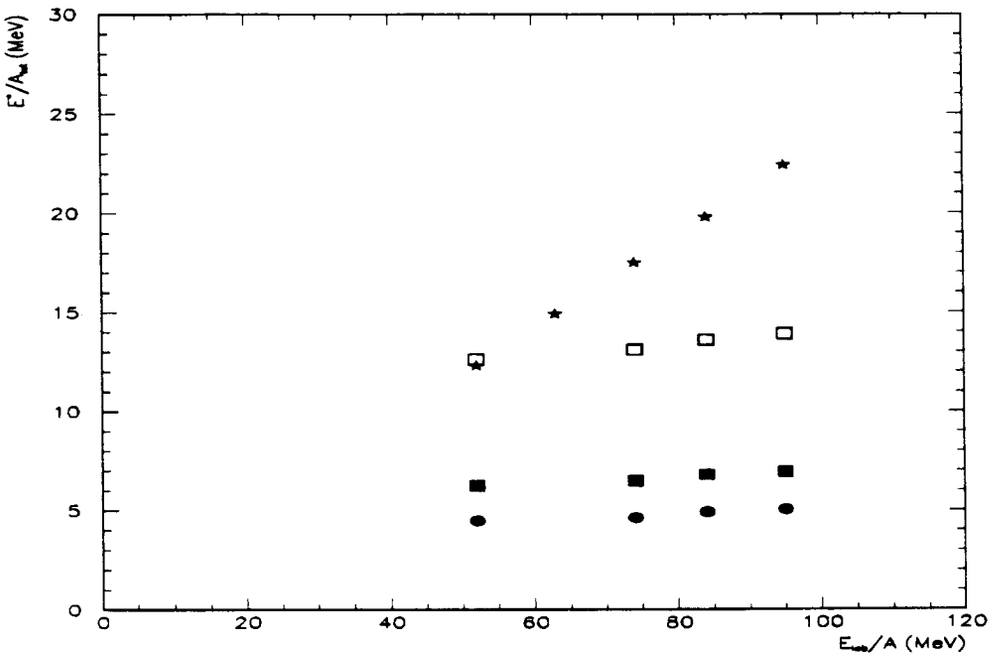

Figure 6 : Evolution of the different components which enter the estimated excitation energy (see text) as compared to the available one (stars).

4. Conclusion

In order to sample the first results obtained with the INDRA detector, the evolution of the $^{36}Ar + ^{58}Ni$ system has been studied. Keeping only the well detected events, a large impact parameter range is selected. This allows to follow the evolution of the involved reaction mechanism over a wide incident energy range : from 32 MeV/A up to 95 MeV/A. The study of IMF , Z, and Z_{max} distributions for different class of impact parameters shows a slow evolution of the reaction mechanism rather than a sudden change at a given energy. The threshold for vaporization of the system is estimated to be around 12 MeV/A excitation energy. Energy calibration energy will be available very soon and will allow to follow this study.

REFERENCES

1. R. Bougault et al., Nucl. Phys. A488(1988)255c.
2. E. Piasecki et al., Phys. Rev. Lett. 66(1991)1291.
3. C.A. Ogilvie et al., Phys. Rev. Lett. 67(1991)1214.
4. D.R. Bowman et al., Phys. Rev. Lett. 67(1991)1527.
5. R.T. de Souza et al., Phys. Lett. B268(1991)6.
6. K. Hagel et al., Phys. Rev. Lett. 68(1992)2141.
7. B. Borderie et al., Proceedings of the XXXI International Winter Meeting on Nuclear Physics (1993)238.
8. J. Pouthas et al., to be submitted to Nucl. Instr. Meth. A , (1994).
9. L.G. Moretto et al., Ann. Rev. Nucl. Part. 43(1993)279, and references therein.
10. E. Suraud et al., Nucl. Phys. A495(1989)73c.
11. E. Suraud et al., Phys. Lett. B229(1989)359.
12. J. Aichelin et al., Phys. Lett. B176(1986)14.
13. S. Levit et al., Nucl. Phys. A347(1985)426.
14. B. Borderie et al., Phys. Lett. B302(1993)15.
15. L.G. Moretto et al., Phys. Rev. Lett. 69(1992)1884.
16. P. Bonche et al. Nucl. Phys. A437(1985)265.
17. J. Bondorf et al., Nucl. Phys. A443(1985)321
    J. Bondorf et al., Nucl. Phys. A444(1985)460.
18. D.H.E. Gross et al., Rep. Prog. Phys. 53(1990)605.
19. S. Kox et al., Nucl. Phys. A420 (1984)162.
    S. Kox, Thèse de l'Universite de Grenoble ISN 85-05 (1985), unpublished.
20. D. Benchekroun, Thèse de l'Universite de Lyon N°9494 (1994), unpublished.
21. B. Borderie, Ann. Phys. 17(1992)349.